http://dx.doi.org/10.5012/bkcs.2012.33.4.1199

CO Oxidation of Catalytic Filters Consisting of Ni Nanoparticles on Carbon Fiber

Hyun Ook Seo, Jong Won Nam, Kwang-Dae Kim, Young Dok Kim,* and Dong Chan Lim†

*Department of Chemistry, Sungkyunkwan University, Suwon 440-746, Korea. *E-mail: ydkim91@skku.edu*
†Materials Processing Division, Korea Institute of Materials Science, Changwon 641-010, Korea
Received December 21, 2011, Accepted January 2, 2012

Catalytic filters consisting of Ni nanoparticle and carbon fiber with different oxidation states of Ni (either metallic or oxidic) were prepared using a chemical vapor deposition process and various post-annealing steps. CO oxidation reactivity of each sample was evaluated using a batch type quartz reactor with a gas mixture of CO (500 mtorr) and O_2 (3 torr) at 300 °C. Metallic and oxidic Ni showed almost the same CO oxidation reactivity. Moreover, the CO oxidation reactivity of metallic sample remained unchanged in the subsequently performed second reaction experiment. We suggested that metallic Ni transformed into oxidic state at the initial stage of the exposure to the reactant gas mixture, and Ni-oxide was catalytically active species. In addition, we found that CO oxidation reactivity of Ni-oxide surface was enhanced by increase in the H_2O impurity in the reactor.

Key Words : Metal : Ni, CO oxidation, Carbon fiber, Chemical vapor deposition

Introduction

Catalytic oxidation of CO to CO_2 has been intensively studied due to its importance in many applications, especially in automobile exhaust treatment devices. In addition, CO oxidation reaction has been used as a model system in fundamental studies to address general scientific questions in heterogeneous catalysis, *i.e.*, determining catalytic mechanism and active site of heterogeneous catalysts.[1-10] Noble-metal catalysts, such as Pt, Ru, Rh and Pd, have been investigated for the several past decades and proven to be catalytically active for CO oxidation.[2-10] In order to understand underlying mechanism and catalytic active site, much effort has been devoted. It has been widely accepted that metallic surfaces of Pt-group metals should be reactive for CO oxidation, whereas the formation of oxide layers on metals reduce CO oxidation reactivity significantly.[2-5] Recent studies, however, suggested that thin oxidic-films on surface of Pt-group catalysts were responsible for CO oxidation reactivity.[6-10]

Recently, oxidative catalysts consisting of Ni have been considered as a promising candidate for applications due to its lower price than other Pt-group metals. Recent studies have shown that Ni has catalytic activity towards CO oxidation at low temperature as well as high temperature.[11-14] Manos and co-workers suggested that low-temperature CO oxidation was catalyzed by NiO(111) surface formed on Ni rather than oxygen adsorbed on Ni(111) surface.[12]

Reactivity of CO oxidation catalyzed by metals can be influenced by humidity, and therefore, systematic studies on change in the reactivity of CO oxidation as a function of H_2O vapor pressure are required. In recent experimental and theoretical works, it has been evidenced that the presence of H_2O vapor can actually be able to promote CO oxidation reaction of various catalysts.[15-17]

In the present work, Ni particles with sizes less than 60 nm were synthesized on carbon fiber filter using pulsed-chemical vapor deposition (CVD) and subsequent vacuum-annealing at 600 °C. CO oxidation reactivity, and the structure of the catalytically active surface of this filter were studied. Influence of the H_2O impurity level on CO oxidation behavior was also studied, and the results will be demonstrated.

Experimental

Sample Preparation. As substrate, carbon fibers purchased from Torray were used, which were about 6-7 μm in mean thickness, and the paper consisting of these carbon fibers were ~170 μm in thickness. NiO particles were deposited on the carbon fiber using pulsed-chemical vapor deposition (CVD) process with $Ni(Cp)_2$ and H_2O precursors. The pulsed-CVD process is different from conventional CVD process in the way that discrete pulses of two precursors are used in a cyclic manner, instead of a continuous flow of precursors. One cycle of pulsed-CVD process consisted of four steps. 1) $Ni(Cp)_2$ precursor with a partial pressure of 1 torr was introduced into the chamber for 300 sec, and then 2) injection of H_2O precursor (70 torr, 10 sec) followed. 3) Sample was exposed to a gas mixture of $Ni(Cp)_2$ and H_2O for 30 sec. 4) After the exposure step, the reactor was purged and evacuated to keep a base pressure of reactor at ~70 mtorr before the next injection of $Ni(Cp)_2$. During NiO deposition process, sample temperature was kept at 280 °C. Temperatures of $Ni(Cp)_2$ and H_2O precursors were kept at 60 °C and room temperature during deposition, respectively. 180 pulsed-CVD cycles were used for preparing NiO/carbon fiber catalysts. After NiO deposition, all the samples were annealed at 600 °C for 1hr in a quartz reactor using furnace under vacuum conditions (base pressure ~8.0×10^{-8} torr). Some of as-prepared samples were

subsequently exposed to oxygen (3 torr, for 30 min, at 300 °C). Surfaces of various samples were analyzed using X-ray photoelectron spectroscopy (XPS) and scanning electron microscopy (SEM). The XPS measurements were performed in the chamber (base pressure ~2×10^{-10} torr) equipped with a concentric hemisphere analyzer (CHA, PHOIBOS-Hsa3500, SPECS) and a dual Al/Mg X-ray source. XPS spectra were obtained at room temperature using Mg Kα-source (1253.6 eV). The binding energies of XPS spectra were referenced using C 1s line at 284.5 eV for adventitious carbon.[18] The morphological image of each sample surface was obtained using SEM (JEOL, JSM7500F).

CO Oxidation Experiments. Experimental set-up used for CO oxidation experiments is schematically described in Figure 1. CO oxidation experiments were carried out in a batch-type quartz reactor (base pressure ~8.0×10^{-8} torr) at 300 °C. Temperature of the quartz reactor could be monitored and controlled by furnace equipped with k-type thermocouple. Catalytic filters consisting of Ni and carbon fiber were placed in the quart tube and the reactor was evacuated using rotary and turbo pump; initially, the chamber was roughly evacuated using rotary pump with closed leak valve "a" and open gate valve "A" (Fig. 1), and then the chamber was further pumped out using turbo pump *via* open leak valve "a" (gate valve "A" was closed during this pumping by turbo pump) (Fig. 1). After a reactor base pressure of ~8.0×10^{-8} torr was reached, leak valve "a" was closed and reactor temperature was increase to 300 °C. Then, 500 mtorr of CO and 3 torr of O_2 were introduced into the chamber at 300 °C *via* leak valves "b" and "c", respectively. During injection of each gas, its pressure could be monitored by a convectron gauge. After injection of a gas mixture of CO and O_2, a gate valve "B" was closed. In every 5 min, small amount of gas in the reactor was introduced into the high-vacuum chamber equipped with a quadrupole mass spectrometer (QMS) *via* leak valve "a" for monitoring change in the relative partial pressures of CO, CO_2, and O_2 in the reactor as a function of time.

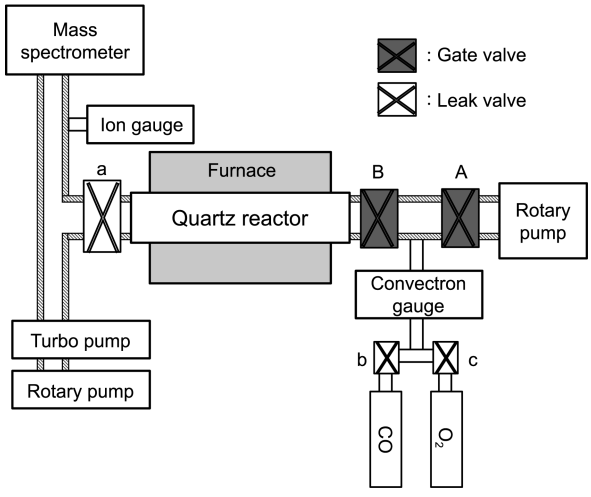

Figure 1. A schematic description of an experimental set-up for CO oxidation experiments is displayed.

Results and Discussions

Characterization. Surface morphology of vacuum-annealed Ni/carbon fiber samples (annealing condition: at 600 °C, for 1hr) and those with a subsequent oxygen treatment (3 torr of O_2, 300 °C, 30 min) were characterized using SEM (Fig. 2). The surface of vacuum-annealed sample (at 600 °C, for 1hr) was covered with Ni particles with a large distribution in their sizes (10 nm ~ 60 nm) (Fig. 2(a))). Upon oxygen exposure, smaller nanoparticles were aggregated, increasing mean size of particles and reducing their size distribution (Fig. 2(b)). Chemical states of Ni in the catalytic filter before and after oxygen treatment were analyzed using XPS (Fig. 3). After vacuum-annealing process, surface of samples were covered mostly with metallic-Ni, as indicated by Ni 2p and O 1s core-level XPS spectra (Fig. 3); only a single peak at 852.2 eV corresponding to metallic-Ni state could be found in Ni $2p_{3/2}$ core level spectra, and there was also no indication of lattice oxygen of oxidic-Ni in O 1s spectra.[18-20] When the sample was subsequently exposed to oxygen, two additional shoulders at 853.4 (NiO) and 855.4 eV, ($Ni(OH)_2$) were appeared, whereas metallic-Ni peak at (853.1 eV) was reduced in intensity (Fig. 3(a)).[18-20] It is notable that the metallic Ni signal did not completely disappear upon the oxygen exposure, *i.e.* NiO thin films with

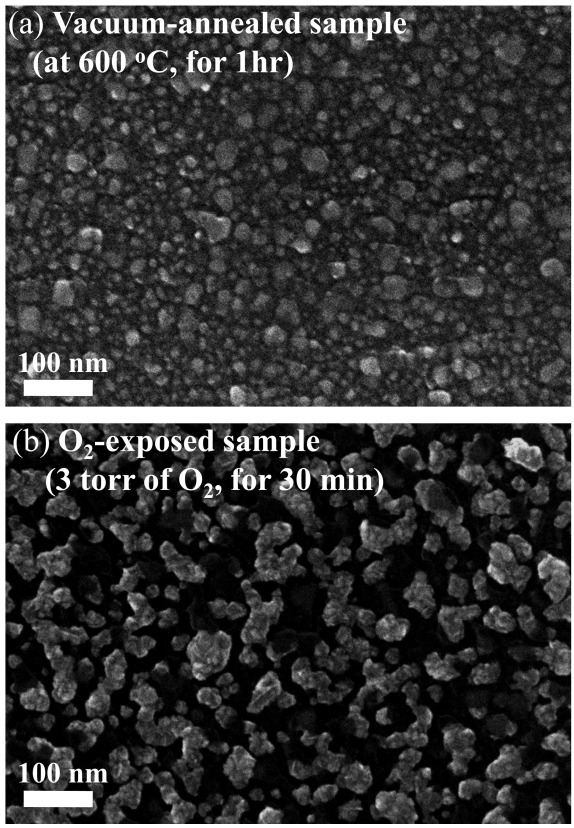

Figure 2. SEM images of samples before CO oxidation reactions are provided; (a) A topological SEM image of a vacuum-annealed sample (at 600 °C, for 1hr) and (b) that of sample prepared with a vacuum-annealing process (at 600 °C, for 1hr) and a subsequent O_2 exposure at 300 °C (3 torr of O_2, for 30 min).

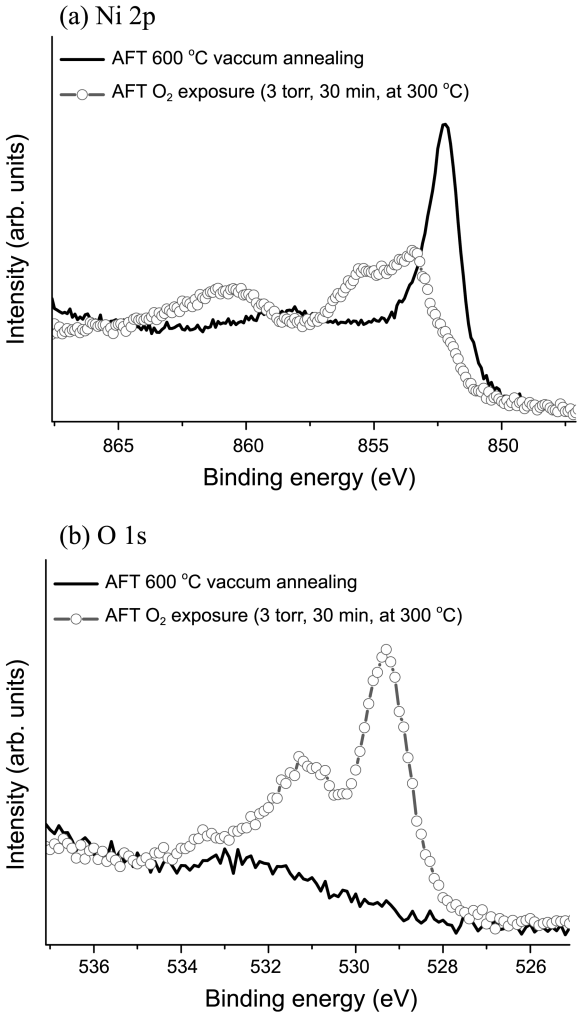

Figure 3. (a) Ni 2p and (b) O 1s core level XPS spectra of vacuum-annealed samples before and after oxygen treatment (at 300 °C, 3 torr of O_2, for 30 min) are compared.

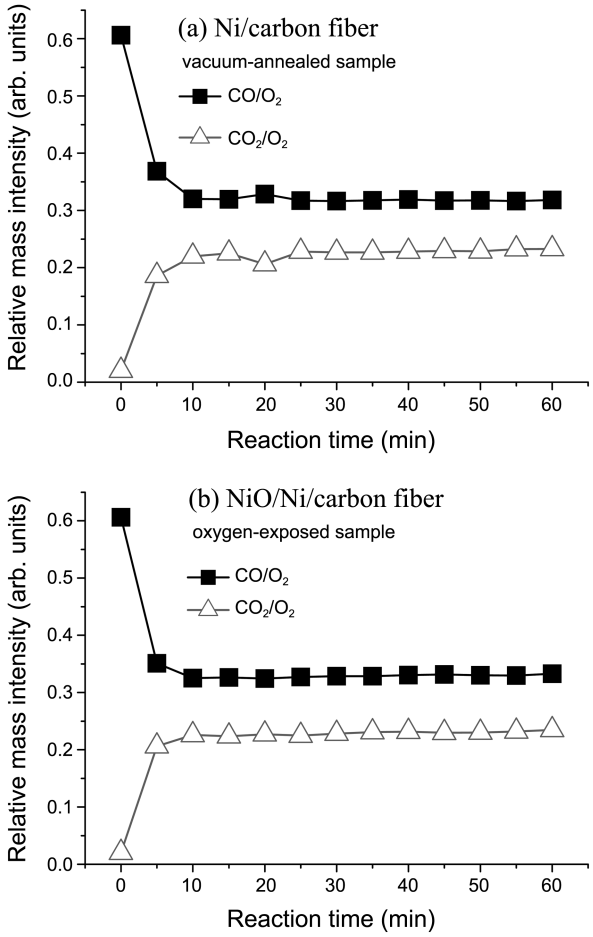

Figure 4. CO oxidation experiments were performed at 300 °C with a gas mixture of 500 mtorr of CO and 3 torr of O_2 in a batch type quartz reactor. With increasing reaction time, changes in the relative mass intensities of CO and CO_2 with respect to O_2 were examined. (a) The catalyst was prepared by a vacuum-annealing process (at 600 °C, for 1hr), and Ni was mostly in the metallic state before reaction. (b) The catalyst was prepared by a vacuum annealing and a subsequent O_2 exposure (at 300 °C, 3 torr of O_2, for 30 min), and Ni was mostly oxidized before reaction.

a thickness less than 4-5 nm formed on Ni core upon oxygen-treatment. In the O 1s core level, appearances of two O 1s peaks at 529.2 and 531.4 eV, which could be ascribed to lattice oxygen of NiO and $Ni(OH)_2$, respectively,[18-20] were observed upon O_2 exposure (Fig. 3(b)).

CO Oxidation Reactivity. CO oxidation reactivity of vacuum-annealed sample with a lateral size of 2 cm^2 was evaluated at a reactor temperature of 300 °C (initial conditions: 500 mtorr of CO and 3 torr of O_2) (Fig. 4(a)). With increasing reaction time, relative mass intensity of CO_2/O_2 was increased, whereas CO/O_2 ratio was decreased, indicating that CO oxidation took place (Fig. 4(a)). We used an excess amount of O_2 with respect to CO, and change in the partial pressure of O_2 during reaction is only a half of that of CO. Therefore, the partial pressure of O_2 during CO oxidation reaction can be regarded as nearly constant. In 10 min, relative mass intensity of CO_2 to O_2 was reached to about 0.22, and there were no further noticeable changes in CO_2/O_2 mass ratio after 10 min (Fig. 4(a)). Under same experimental conditions, CO oxidation reactivity of the sample prepared by vacuum-annealing and subsequent O_2 exposure was examined (Fig. 4(b)). Oxygen-treated sample showed almost the same CO oxidation reactivity with that without oxygen-treatment in terms of initial reaction rate as well as total CO_2 conversion (Fig. 4). Oxygen pre-treatment did not affect CO oxidation reactivity of the catalyst, although the surface structure of the catalyst was completely changed from metallic Ni to thin oxidic-NiO films by the oxygen-treatment.

Figure 5 a shows Ni 2p core level spectra of vacuum-annealed sample obtained before and after CO oxidation reaction. After reaction, only two oxidic-Ni states (NiO at 853.4 eV and $Ni(OH)_2$ at 855.4 eV)[18-20] could be identified in Ni 2p core-level XPS spectra without any noticeable peak at 853.1 eV (metallic-Ni).[18-20] It is worth mentioning that the surface of oxygen-treated sample was also oxidized after CO oxidation, resulting in an increase in a thickness of oxidic-Ni film on its surface; metallic Ni peak (852.2 eV) of oxygen-treated sample, remained upon oxygen-treatment, was com-

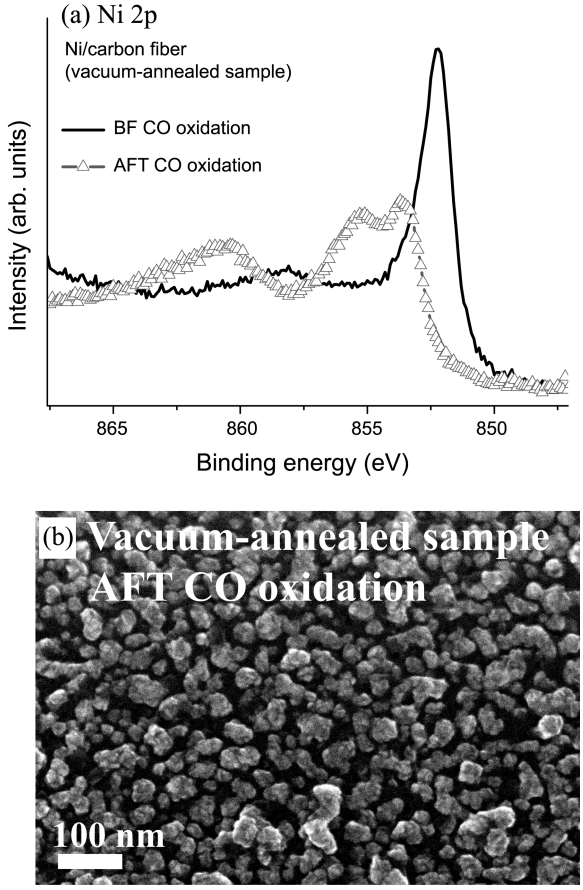

Figure 5. (a) Ni 2p core level XPS spectra of vacuum-annealed samples before and after CO oxidation are compared. (b) A topological SEM image of a vacuum-annealed sample after the CO oxidation is shown.

pletely disappeared after CO oxidation (data were not shown).

After CO oxidation reaction of the vacuum-annealed sample, the aggregation of smaller nanoparticles of Ni and decrease in the particle size distribution could be observed using SEM (Fig. 5(b)). Change in the surface morphology upon CO oxidation reaction is almost similar to that observed after oxygen-treatment in Figure 1.

CO oxidation reaction of the vacuum-annealed sample was repeatedly carried out under same experimental conditions (Fig. 6). The result of the 2nd reaction was almost same as that of the 1st one, and also with the result of CO oxidation with oxygen-treated sample (Fig. 4(b)). It can be suggested that oxidic-Ni films were formed on sample surface of metallic Ni immediately after exposure to gas mixture (at 300 °C, CO and O_2), and then CO oxidation reaction was catalyzed by oxidic-nickel films. Further investigations on changes in oxidation state of Ni oxide upon exposure of CO and O_2 are under way using *in-situ* XPS system, in order to shed light on the mechanism of CO oxidation on oxidic-Ni surface.

During CO oxidation reactions, there were always H_2O impurities in the reactor with a relative mass ratio of about 0.13 with respect to that of O_2. Recently, it has been demonstrated that humidity in the reactor could affect to the

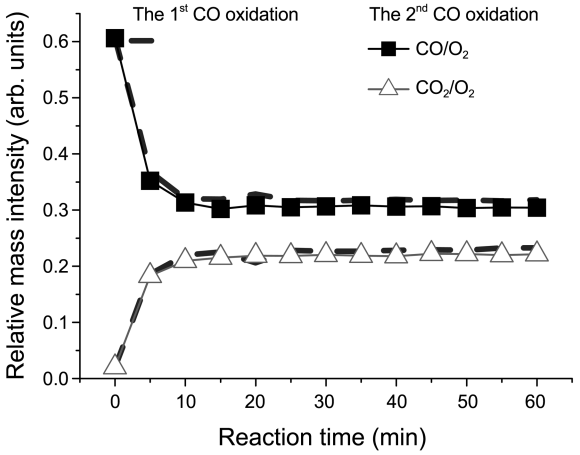

Figure 6. With a vacuum-annealed sample (at 600 °C, for 1hr), CO oxidation reaction was repeatedly performed under same experimental conditions (at 300 °C, 500 mtorr of CO and 3 torr of O_2). The result of the 2nd CO oxidation reaction (relative mass intensities of CO and CO_2 with respect to O_2) with a vacuum-annealed sample is compared of that of the 1st reaction.

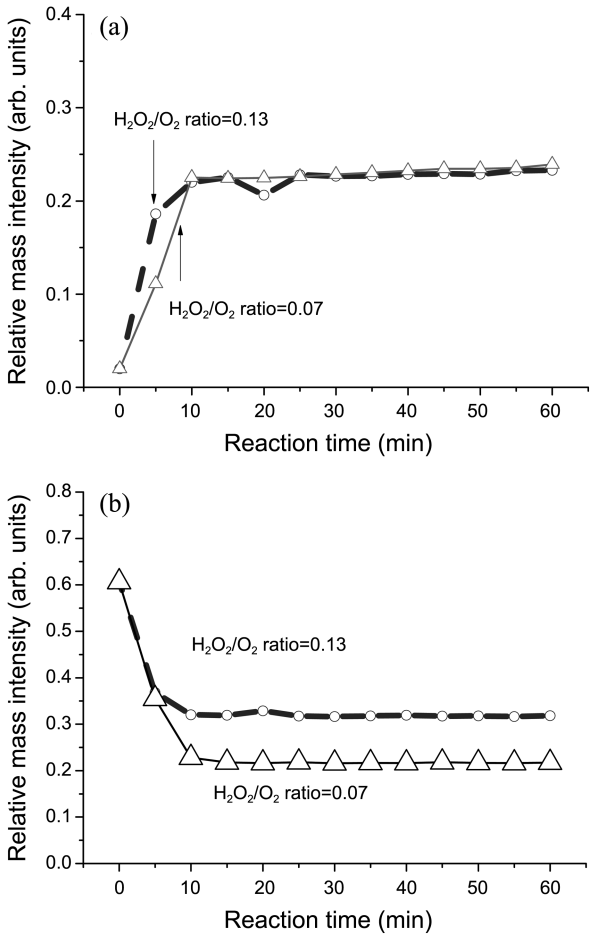

Figure 7. Effect of H_2O impurity level on catalytic reactivity of vacuum-annealed samples (at 600 °C, for 1hr) towards CO oxidation was investigated. H_2O/O_2 ratios in the mass spectra were 0.13 to 0.07, respectively, for two different experimental conditions. (a) CO_2/O_2 ratio change as a function of time was measured for two different water vapor pressire (b) CO/O_2 ratio.

CO oxidation reactivity of catalysts.[15-17] In order to see effects of H_2O impurities on catalytic reactivity, additional CO oxidation experiments were performed in the chamber with a less amount of H_2O impurity. Before injection of the reactant gas mixture (CO and O_2), extra pumping (for 12 hrs, using turbo and rotary pump) was applied to reduce H_2O impurity level in the reactor. Relative mass intensity of H_2O to O_2 was decreased to 0.07 from 0.13 upon the extra pumping. With a less amount of H_2O vapor inside the chamber, initial CO_2 production rate was decreased by a factor of 2 (Fig. 7), indicating that presence of H_2O vapor in the reactor could promote CO oxidation reactivity of catalysts. It is notable that the CO partial pressure initially more steeply decreased under the experimental conditions of lower amount of H_2O: when the partial pressure of H_2O was lower (0.07), CO_2 formation was slower, whereas initial CO removal rate was much faster. This result implies that CO removal was enhanced by adsorption of CO on the surface of catalysts when the H_2O vapor pressure was lower, *i.e.* adsorption of water and CO could be competitive. One can conclude that H_2O vapor increased CO_2 formation rate and removed CO adsorption on the surface of catalyst. It has been reported that water molecules could facilitate formation of activated oxygen species on catalyst surfaces, thereby increasing the catalytic reactivity for CO oxidation.[15-17] This previous results are in line with our data in Figure 7.

Conclusions

In the present work, carbon filters covered with Ni nanoparticles (10-60 nm) were synthesized using a pulsed-CVD process with $Ni(Cp)_2$ and H_2O precursors and a subsequent annealing (at 600 ^oC, for 1hr) in a vacuum chamber (~8.0×10^{-8} torr). On this surface, Ni mostly existed in the metallic state. Upon subsequent exposure of this sample to 3 torr of O_2 at 300 ^oC for 30 min, oxidic-Ni films (< 5 nm), consisting of NiO and $Ni(OH)_2$, were formed. Two different samples, without and with NiO thin films on their surface, respectively, showed almost same CO oxidation reactivities at 300 ^oC. In a repeatedly performed CO oxidation experiments using the same catalyst, no change in the CO oxidation reactivity could be found, *i.e.* the reactivity in the 2nd experiment was identical to that of the 1st ones. One can suggest that originally metallic Ni catalysts transformed oxidic-Ni state upon exposure to a reagent gas mixture (CO and O_2), and the oxidic-Ni was responsible for CO oxidation reactivity. Catalytic reactivity of vacuum-annealed sample was also evaluated in the reactor with different levels of H_2O impurity, and increase in the CO reactivity with increasing water vapor was found. Our result implies that humidity is an important factor for determining catalytic activity of Ni-based catalysts.

Acknowledgments. This research was supported by a grant from the Fundamental R&D Program for Core Technology of Materials funded by the Ministry of Knowledge Economy, Republic of Korea.

References

1. Ertl, G. *Adv. Catal*. **2000**, *45*, 1.
2. Chen, M. S.; Wang, X. V.; Zhang, L. H.; Tang, Z. Y.; Wan, H. L. *Langmuir* **2010**, *26*, 18113.
3. Gao, F.; Goodman, D. W. *Langmuir* **2010**, *26*, 16540.
4. Gao, F; Wang, Y.; Cai, Y.; Goodman, D. W. *J. Phys. Chem.* **2009**, *113*, 174.
5. McClure, S. M.; Goodman, D. W. *Chem. Phys. Lett.* **2009**, *469*, 1.
6. Ackermann, M. D.; Pedersen, T. M.; Hendriksen, B. L. M.; Robach, O.; Bobaru, S. C.; Popa, I.; Quiros, C.; Kim, H.; Hammer, B.; Ferrer, S.; Frenken, J. W. M. *Phys. Rev. Lett.* **2005**, *95*, 4.
7. Grass, M. E.; Zhang, Y. W.; Butcher, D. R.; Park, J. Y.; Li, Y. M.; Bluhm, H.; Bratlie, K. M.; Zhang, T. F.; Somorjai, G. A. *Angew. Chem. Int. Ed.* **2008**, *47*, 8893.
8. Hendriksen, B. L. M.; Frenken, J. W. M. *Phys. Rev. Lett.* **2002**, *89*, 4.
9. Over, H.; Balmes, O.; Lundgren, E. *Surf. Sci.* **2009**, *603*, 298.
10. Over, H.; Kim, Y. D.; Seitsonen, A. P.; Wendt, S.; Lundgren, E.; Schmid, M.; Varga, P.; Morgante, A.; Ertl, G. *Science* **2000**, *287*, 1474.
11. Knudsen, J.; Merte, L. R.; Peng, G. W.; Vang, R. T.; Resta, A.; Laegsgaard, E.; Andersen, J. N.; Mavrikakis, M.; Besenbacher, F. *Acs Nano*. **2010**, *4*, 4380.
12. Peng, G. W.; Merte, L. R.; Knudsen, J.; Vang, R. T.; Laegsgaard, E.; Besenbacher, F.; Mavrikakis, M. *J. Phys. Chem. C* **2010**, *114*, 21579.
13. Zhao, B.; Ke, X.-K.; Bao, J.-H.; Wang, C.-L.; Dong, L.; Chen, Y.-W.; Chen, H.-L. *J. Phys. Chem. C* **2009**, *113*, 14440.
14. Wang, D. S.; Xu, R.; Wang, X.; Li, Y. D. *Nanotechnol.* **2006**, *17*, 979.
15. Rajasree, R.; Hoebink, J. H. B. J.; Schouten, J. C. *J. Catal.* **2004**, *223*, 36.
16. Gong, X. *J. Chem. Phys.* **2003**, *119*, 6324.
17. Bergeld, J.; Kasemo, B.; Chakarov, D. V. *Surf. Sci.* **2001**, *495*, L815.
18. Moulder, J. F.; Stickle, W. F.; Sobol, P. E.; Bomben, K. D. *Hankbook of X-ray Photoelectron Spectroscopy*; Chastain, J., King, R. C., Jr., Eds.; Physical Electronics, Inc: Minnesota, U.S.A., 1995.
19. Greiner, M. T.; Helander, M. G.; Wang, Z.-B.; Tang, W.-M.; Lu, Z.-H. *J. Phys. Chem. C* **2010**, *114*, 19777.
20. Biesinger, M. C.; Payne, B. P.; Lau, L. W. M.; Gerson, A.; Smart, R. S. C. *Surf. Interf. Anal.* **2009**, *41*, 324.